DALTON

Polynuclear pyrazolato complexes. Synthesis, chemical reactivity and crystal structures of $[\{Pd(dmpz)_2(Hdmpz)_2\}_2]$ and $[\{PdAg_2(dmpz)_4\}_2]$ (Hdmpz = 3,5-dimethylpyrazole)

G. Attilio Ardizzoia,*[a] Girolamo La Monica,[a] Sergio Cenini,[a] Massimo Moret*[b] and Norberto Masciocchi[b]

[a] *Dipartimento di Chimica Inorganica, Metallorganica ed Analitica e Centro CNR, Università di Milano, Via Venezian 21, 20133 Milano, Italy*
[b] *Dipartimento di Chimica Strutturale e Stereochimica Inorganica, Università di Milano, via Venezian 21, 20133 Milano, Italy*

The dinuclear complex $[\{Pd(dmpz)_2(Hdmpz)_2\}_2]$ (Hdmpz = 3,5-dimethylpyrazole) has been synthesized and its solid-state structure determined by X-ray methods. Each dimeric molecule, of idealized 422 symmetry, possesses four strong intramolecular hydrogen bonds, equalizing the Hdmpz and dmpz ligands. The complex has been treated with $AgNO_3$ and $[Cu(MeCN)_4]BF_4$, in search of heterobimetallic derivatives; $[\{PdCu_2(dmpz)_4\}_2]$ and $[\{PdAg_2(dmpz)_4\}_2]$ species have been isolated. The latter, characterized by X-ray methods, is a non-bonded octahedral cluster (*trans* Pd_2Ag_4) bridged by eight dihapto dmpz ligands, thus formally deriving from its precursor by substitution of four H^+ by Ag^+ ions. This increases the Pd ··· Pd distance from 3.746(1) to 5.160(1) Å, and slightly changes the ligand conformation.

Pyrazole-type heterocycles represent an important class of ligands in co-ordination chemistry.[1] They can act as neutral monodentate (pyrazole-*N*), anionic monodentate (pyrazolato-*N*) or *exo*- or *endo*-bidentate[2] anionic ligands (pyrazolato-*N*,*N*'). We have been particularly interested in the synthesis, structural characterization, reactivity and catalytic properties of copper(I) and silver(I) complexes containing *exo*-bidentate pyrazolate ligands.[3] Our interest has been focused on the ability of copper(I) pyrazolato complexes of general formula $[\{Cu(3,5R_2\text{-}pz)\}_n]$ (R = Me, n = 3; R = Ph, n = 4) to act as selective catalysts in the oxidation of organic substrates such as aromatic or aliphatic amines.[4]

It is well known that platinum-group metals exhibit a very rich co-ordination chemistry and their catalytic properties have attracted much attention. Moreover, the potential role of polynuclear metal complexes has prompted many authors to synthesize and test a large number of such systems. With this aim, the synthesis of a number of polynuclear pyrazolato complexes of Ni^{II}, Pd^{II} and Pt^{II} have been reported recently. In particular, the preparation and crystal structure of a platinum(II) complex of formula $[\{Pt(pz)_2(Hpz)_2\}_2]$ (Hpz = pyrazole) has been published.[5]

In this paper we report the synthesis and the characterization of the isostructural palladium(II) complex $[\{Pd(dmpz)_2(Hdmpz)_2\}_2]$ **1** (Hdmpz = 3,5-dimethylpyrazole). The ability of this species to act as a bedrock for the preparation of heterobimetallic species was verified. In particular, the synthesis and structural characterization of the hexanuclear bimetallic species $[\{PdAg_2(dmpz)_4\}_2]$ is reported.

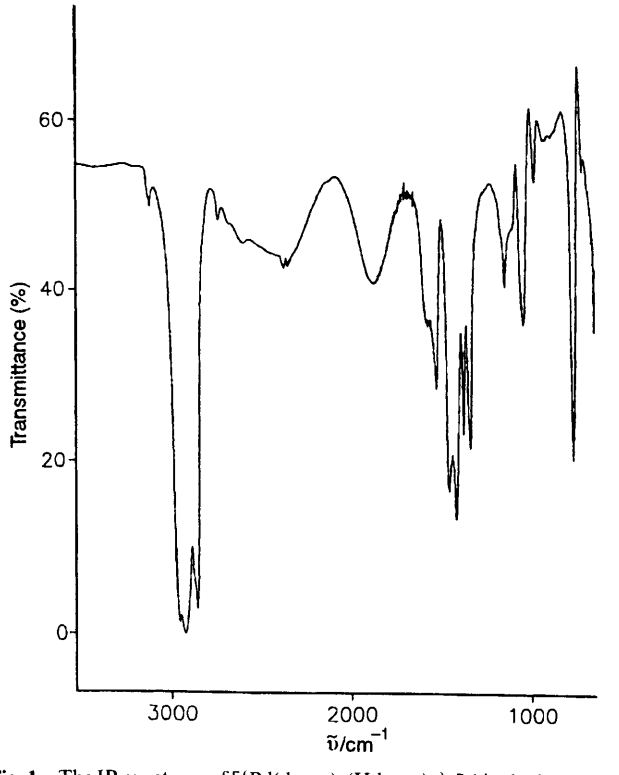

Fig. 1 The IR spectrum of $[\{Pd(dmpz)_2(Hdmpz)_2\}_2]$ **1** in the 3500–650 cm^{-1} region (Nujol mull)

Results and Discussion

The complex $[PdCl_2(MeCN)_2]$ reacts with an excess of 3,5-dimethylpyrazole (Hdmpz) in methanol in the presence of NEt_3, giving the new pyrazolepyrazolatopalladium(II) complex $[\{Pd(dmpz)_2(Hdmpz)_2\}_2]$ **1** as an insoluble white product. The same species can be obtained by treating $PdCl_2$ or $Na_2[PdCl_4]$ with an excess of Hdmpz in the presence of triethylamine in water.

The IR spectrum of complex **1** is shown in Fig. 1. The most striking feature is the presence of broad bands centred at 2500 and 1850 cm^{-1}. The first absorption can easily be attributed to the presence of N–H ··· N hydrogen bonds. Such a band has been reported for complexes containing pyrazole and pyrazolato groups interacting through hydrogen bonds *e.g.* the platinum(II) complex $[Pt(pz)_2(Hpz)_2]$,[5] isostructural with **1**, or $[Ir(\eta^5\text{-}C_5Me_5)(pz)_2(Hpz)]$.[6] On the contrary, the absorption of **1** at 1850 cm^{-1} is not so easily assignable. The IR spectra of somewhat related dimeric species, $[Zn_2(dmpz)_4(Hdmpz)_2]$[7]

and $[Co_2(dmpz)_4(Hdmpz)_2]$,[8] show two broad bands at about 2380 and 1860 cm^{-1}, and the isostructural platinum(II) complex $[Pt(pz)_2(Hpz)_2]$,[5] which we prepared for a useful comparison, also exhibits a similar pattern, even though the authors did not mention it. It is worth noting that IR studies performed at low temperatures (−160 °C) on crystals of $HClO_4 \cdot 3H_2O$ and $HNO_3 \cdot 3H_2O$ showed strong absorptions at 2600 and 1900 cm^{-1}.[9] The latter has been explained in terms of Fermi resonance between the ν(O–H · · · O) and the overtone 2δ(O–H · · · O). Further studies are necessary in order to extrapolate such results to our N–H · · · N system. Attempts made to prepare the deuteriated species $[\{Pd(dmpz)_2([^2H]\text{-}Hdmpz)_2\}_2]$ by deuteriation of **1** have been unsuccessful.

A crystal structure determination for complex **1** has been performed. Consistent with the IR spectrum, it revealed the presence of two monomeric $Pd(dmpz)_2(Hdmpz)_2$ units linked by four symmetrical N–H · · · N bridges between the Hdmpz and $dmpz^-$ ligands.

Crystal and molecular structure of complex 1

The crystals of $[\{Pd(dmpz)_2(Hdmpz)_2\}_2]$ contain Pd^{II} co-ordinated, in a square-planar environment, by four nitrogen atoms of four distinct (formally two 3,5-dimethylpyrazole and two 3,5-dimethylpyrazolate) ligands [*cis* N–Pd–N values lie in the range 89.4(1)–91.0(1)°]. Selected distances and angles are collected in Table 1. The Pd–N values (average 2.014 Å, typical estimated standard deviation, e.s.d. = 0.002 Å) and ring sizes fall within the normal ranges observed for similar compounds. Each PdL_4 moiety lies close to a crystallographic two-fold axis, giving rise to dimeric, rather than monomeric, molecules.

Although the Pd · · · Pd contact is rather long [3.746(1) Å], definitely indicating the absence of any direct metal–metal interaction, the dimeric nature of the molecule is ensured by the four strong N–H · · · N hydrogen bonds observed between pyrazole and pyrazolato rings connected to different Pd atoms [N · · · N 2.704(4) and 2.692(4) Å]. The correct position of the bridging H atoms could not be detected experimentally from our diffraction data, but, as already observed in other (fully organic) N(pyrazole)–H · · · N(pyrazole) interactions,[10] the H atoms are likely to be disordered in two different, but equally populated, sites, making all heterocyclic rings equivalent; however, the possibility of a single minimum potential along the N · · · N contacts, such as that evidenced from neutron diffraction data of 3-methylphenylpyrazole, cannot be discarded.[11]

With reference to Fig. 2, where the whole dimeric molecule is drawn and a partial atomic labelling scheme added, it can be seen that $[\{Pd(dmpz)_2(Hdmpz)_2\}_2]$ possesses idealized 422 (D_4) symmetry, with the four-fold axis passing through the metal atoms and two different sets of two-fold axes normal to it, one of which passes through the midpoints of opposite N–H · · · N interactions. The point-group symmetry indicates that each dimer is a chiral molecule, with a four-fold propeller-like shape, crystallizing, as a racemate, in the centric space group *C*2/*c*. The same molecular arrangement has been previously found in $[Pt(pz)_2(Hpz)_2]$,[5] and indicates that this ligand disposition, maximizing the intramolecular hydrogen-bond interactions, is a common motif of these species; however, in the platinum derivative, a much shorter metal–metal contact is observed (3.370 Å).* Analogously, $[PdCl_2(Hdmpz)_2]$ shows, in the solid state, dimeric moieties with strong N–H · · · Cl interactions of idealized D_2 (222) symmetry.[13]

The repeated observations of such a pairing effect within this class of compounds suggest that, probably, the dimeric nature is maintained in low-polarity solvents, where dissociation, *i.e.* simultaneous breaking of four hydrogen bonds, is not likely to occur. Therefore, we formulate all aforementioned complexes as dimeric species. Consistently, the IR spectrum of **1** in CH_2Cl_2 solution shows the same pattern of NH absorptions as those exhibited in the solid state. Complex **1** revealed high rigidity even in solution, not showing any fluxional behaviour as indicted by variable-temperature ^1H NMR measurements. In the range −80 to 40 °C the ^1H NMR spectrum (CD_2Cl_2 solutions) did not show any noticeable modification. Four signals are detectable at δ 1.71, 1.75, 5.44 and 18.1. The first three are attributable to the methyl substituents in the 3,5 positions of the pyrazole rings and to the C(4)H proton, respectively. The presence of a single signal attributable to latter hydrogen strongly supports the equivalence of the Hdmpz and $dmpz^-$ ligands. The signal at δ 18.1 is assignable to the NH protons involved in the intramolecular hydrogen bonds. This signal is found at very low field, when compared with the position of the NH proton in free Hdmpz (δ 10.8) and in the pyrazole pyrazolate complex $[Ir(\eta^5C_5Me_5)(dmpz)\text{-}(Hdmpz)_2]BF_4$ (δ 10.4).[6]

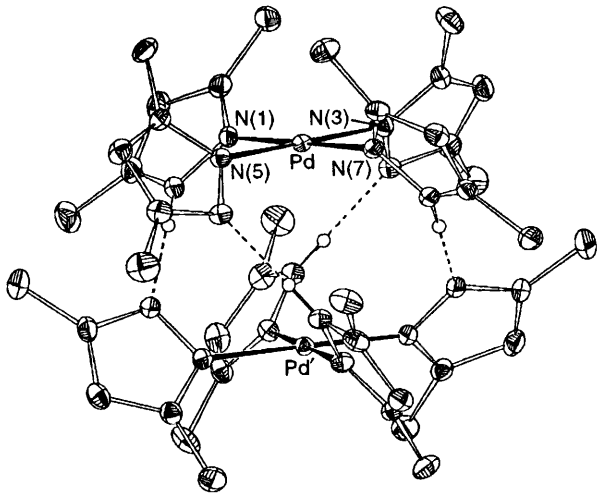

Fig. 2 An ORTEP[12] drawing of the $[\{Pd(dmpz)_2(Hdmpz)_2\}_2]$ molecule, with partial labelling scheme. Thermal ellipsoids are drawn at the 30% probability level. Only one set of disordered, N,N bridging H atoms is shown for clarity

Table 1 Selected bond lengths (Å) and angles (°) for complex **1**

Pd–N(1)	2.020(2)	C(1)–C(2)	1.390(5)
Pd–N(3)	2.015(2)	C(1)–C(4)	1.491(5)
Pd–N(5)	2.012(2)	C(2)–C(3)	1.378(5)
Pd–N(7)	2.008(2)	C(3)–C(5)	1.493(5)
N(1)–C(1)	1.347(4)	C(6)–C(7)	1.375(5)
N(1)–N(2)	1.359(3)	C(6)–C(9)	1.496(5)
N(2)–C(3)	1.347(4)	C(7)–C(8)	1.384(5)
N(3)–C(6)	1.347(4)	C(8)–C(10)	1.498(5)
N(3)–N(4)	1.361(3)	C(11)–C(12)	1.383(5)
N(4)–C(8)	1.342(4)	C(11)–C(14)	1.487(5)
N(5)–C(11)	1.343(4)	C(12)–C(13)	1.377(5)
N(5)–N(6)	1.358(3)	C(13)–C(15)	1.496(5)
N(6)–C(13)	1.343(4)	C(16)–C(17)	1.377(4)
N(7)–C(16)	1.351(4)	C(16)–C(19)	1.498(5)
N(7)–N(8)	1.362(3)	C(17)–C(18)	1.386(5)
N(8)–C(18)	1.343(4)	C(18)–C(20)	1.494(5)
N(1)–Pd–N(3)	91.04(10)	N(3)–Pd–N(5)	178.98(9)
N(1)–Pd–N(5)	89.51(10)	N(3)–Pd–N(7)	90.08(10)
N(1)–Pd–N(7)	178.73(10)	N(5)–Pd–N(7)	89.36(10)

Thermolysis of complex 1

A thermogravimetric analysis carried out on complex **1** showed its stability up to 240 °C. A further increase in temperature causes a rapid weight loss of about 40%. Complete

* Using X-ray powder diffraction, we have also shown that $[Pd(pz)_2(Hpz)_2]$ is isomorphous with $[Pt(pz)_2(Hpz)_2]$.

decomposition was observed at temperatures higher than 350 °C. When the heating was stopped at 240 °C a pale yellow palladium(II) complex, analysing as $Pd(dmpz)_2$, was recovered. These results can be interpreted in terms of reaction (1). Similar

$$n[\{Pd(dmpz)_2(Hdmpz)_2\}_2] \longrightarrow 2[\{Pd(dmpz)_2\}_n] + 2n\,Hdmpz \quad (1)$$

thermal behaviour was observed in the cases of $[\{Pd(pz)_2(Hpz)_2\}_2]$ and $[Zn_2(dmpz)_4(Hdmpz)_2]$,[7] palladium and zinc being recovered as the pyrazolate derivatives $[\{Pd(pz)_2\}_n]$ and $[\{Zn(pz)_2\}_n]$, respectively.

A palladium(II) pyrazolate having the same formulation, $[\{Pd(pz)_2\}_n]$, has been reported.[14] It was obtained employing a completely different synthetic route, and was formulated as a polymeric species.

Concerning the nuclearity of $[\{Pd(dmpz)_2\}_n]$ our previous studies on a series of copper(I) and silver(I) pyrazolates confirmed that their nuclearity is strongly dependent on the synthetic methods.[4,15] Moreover, it has been demonstrated by other authors and by us that homoleptic complexes containing the simple pyrazolato group or pyrazolato groups substituted at the 4 position may give rise to polymeric structures.[16] On the contrary, only oligomeric species have been structurally characterized when the pyrazolato group was substituted in the 3,5 positions.[17] On the basis of these observations, we propose for $[\{Pd(dmpz)_2\}_n]$ an oligomeric nature (possibly trimeric in analogy with palladium(II) acetate[18] and $[\{Pt(pz)_2\}_3]$[19]).

Mechanism of formation of complex 1

Since the simplest mode of co-ordination of pyrazole and its derivatives is as a neutral ligand, giving place to derivatives like $M(Hpz^*)_nX_m$ (M = transition metal; X = Cl, Br, I, NO_3 or SO_4; Hpz* = a generic pyrazole),[20] it was reasonable to suppose that the mechanism of formation of complex **1** may involve, as the first step, the formation of a palladium(II) species containing neutral Hdmpz ligands. Indeed, we verified that $[PdCl_2(MeCN)_2]$ easily reacts with an excess of Hdmpz in diethyl ether affording a white crystalline solid analysing as $PdCl_2(Hdmpz)_3$. On the basis of the well known tendency of palladium(II) to maintain a square-planar geometry, we originally formulated this derivative as a ionic species, *i.e.* $[PdCl(Hdmpz)_3]Cl$ **2**. However, complex **2**, in solution, did not show any ionic character, as revealed by conductivity measurements. This behaviour is understandable on the basis of the pronounced tendency of **2** to dissociate Hdmpz ligands giving a species analysing as $PdCl_2(Hdmpz)$, probably dimeric, *i.e.* $[(Hdmpz)ClPd(\mu\text{-}Cl)_2PdCl(Hdmpz)]$ **3**, in analogy with $[(lut)ClPt(\mu\text{-}Cl)_2PtCl(lut)]$(lut = 2,6-lutidine, *i.e.* 2,6-dimethylpyridine)[21] [equation (2)]. Repeated attempts to grow crystals

$$2\,[PdCl(Hdmpz)_3]Cl \longrightarrow [(Hdmpz)ClPd(\mu\text{-}Cl)_2PdCl(Hdmpz)] + 4\,Hdmpz \quad (2)$$

of species **2** failed. In all cases complex **3** was recovered.

As expected, the number of neutral pyrazoles co-ordinated to the palladium(II) centre is related to the steric hindrance of the pyrazole itself. In fact, when treated with $[PdCl_2(MeCN)_2]$, Hpz and Hdppz (3,5-diphenylpyrazole) gave $[Pd(Hpz)_4]Cl_2$ **4** and $[PdCl_2(Hdppz)_2]$ **5**, respectively. Whilst **5** maintains its identity in solution, the behaviour of **4** was confirmed to be identical to that of **2**.

The intermediacy of $[PdCl(Hdmpz)_3]Cl$ in the formation of $[\{Pd(dmpz)_2(Hdmpz)_2\}_2]$ is evidenced by the observation that complex is **2** converted quantitatively into **1** when treated with NEt_3 in the presence of free Hdmpz [equation (3)]. When reaction (3) was carried out in the absence of free Hdmpz a mixture of two palladium(II) species was obtained [equation (4)]. The already known *trans*-$[PdCl_2(Hdmpz)_2]$[13] can be

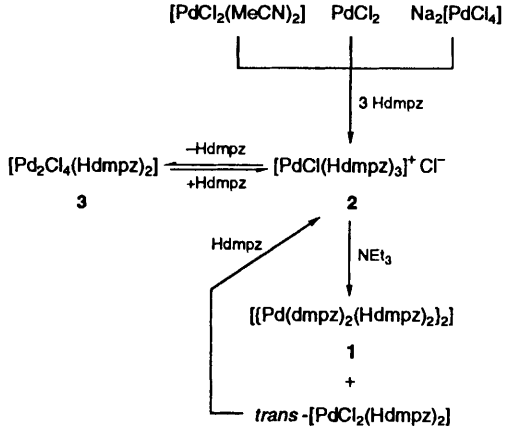

Scheme 1

$$2\,[PdCl(Hdmpz)_3]Cl \xrightarrow[-[NEt_3H]Cl]{NEt_3,\ Hdmpz} [\{Pd(dmpz)_2(Hdmpz)_2\}_2] \quad (3)$$

$$2\,[PdCl(Hdmpz)_3]Cl \xrightarrow[-[NEt_3H]Cl]{NEt_3} [\{Pd(dmpz)_2(Hdmpz)_2\}_2] + trans\text{-}[PdCl_2(Hdmpz)_2] \quad (4)$$

converted into **1** with further Hdmpz in the presence of NEt_3. The aforementioned steps can be usefully summarized by Scheme 1.

Synthesis of heterohexanuclear derivatives

The complex $[\{Pd(dmpz)_2(Hdmpz)_2\}_2]$ **1** readily reacts with $AgNO_3$ in acetonitrile, affording a white crystalline product, later characterized as the heterohexanuclear complex $[\{PdAg_2(dmpz)_4\}_2]$ **6** [equation (5)]. The IR spectrum of **6** shows

$$[\{Pd(dmpz)_2(Hdmpz)_2\}_2] + 4\,AgNO_3 \longrightarrow [\{PdAg_2(dmpz)_4\}_2] + 4\,HNO_3 \quad (5)$$

absorptions corresponding to the dmpz ligands and the disappearance of the N–H bands of the starting material. The ^1H NMR spectrum (CD_2Cl_2) at room temperature shows only one type of pyrazolate environment [δ 1.85, 1.89, Me; δ 5.66, C(4)H]. This pattern is not affected by lowering the temperature. Thus, the behaviour of **6** strongly resembles that of complex **1**. The crystal structure revealed the close analogy between complexes **6** and **1**; indeed, the latter can be thought as derived by a formal substitution of the isolobal H^+ and Ag^+ fragments (see later).

Complex **1** was treated with $[Cu(MeCN)_4]BF_4$ in acetonitrile with the aim of obtaining the copper analogue of **6**, $[\{PdCu_2(dmpz)_4\}_2]$. Using the same experimental conditions, no reaction was observed. A complex analysing as $PdCu_2(dmpz)_4$ **7** was obtained when NEt_3 was added to the reaction mixture [equation (6)]. The synthesis of complex **6** did

$$[\{Pd(dmpz)_2(Hdmpz)_2\}_2] + 4\,[Cu(MeCN)_4]BF_4 \xrightarrow{NEt_3} [\{PdCu_2(dmpz)_4\}] + 4\,[NEt_3H]BF_4 + 4\,MeCN \quad (6)$$

not require the presence of any base. The IR spectrum of **7**, in the 4000–600 cm^{-1} region, is quite similar to that of **6**; also in this case no ν(NH) absorptions are present. The high sensitivity of this Pd^{II}–Cu^{I} derivative to air and moisture, even in the solid state, made a detailed solution study troublesome. However, the similarity between the IR spectra of **7** and **6** seems to suggest a strict analogy (also structural).

Crystal and molecular structure of complex 6

Substitution of the four bridging hydrogen atoms with the

Table 2 Selected bond lengths (Å) and angles (°) for complex **6**

Pd–N(1)	2.008(3)	N(7)–C(16)	1.347(5)
Pd–N(3)	2.012(3)	N(7)–N(8)	1.360(4)
Pd–N(5)	2.016(3)	N(8)–C(18)	1.344(5)
Pd–N(7)	2.017(3)	C(1)–C(2)	1.373(6)
Ag(1)···Ag(1^{I})	3.310(1)	C(1)–C(4)	1.493(5)
Ag(2)···Ag(2^{I})	3.306(1)	C(2)–C(3)	1.383(6)
Ag(1)–N(2)	2.081(3)	C(3)–C(5)	1.497(6)
Ag(1)–N(4^{I})	2.076(3)	C(6)–C(7)	1.377(6)
Ag(2)–N(6)	2.083(3)	C(6)–C(9)	1.502(6)
Ag(2)–N(8^{I})	2.086(3)	C(7)–C(8)	1.377(6)
N(1)–C(1)	1.346(5)	C(8)–C(10)	1.496(6)
N(1)–N(2)	1.367(4)	C(11)–C(12)	1.375(6)
N(2)–C(3)	1.337(5)	C(11)–C(14)	1.490(6)
N(3)–C(6)	1.334(5)	C(12)–C(13)	1.384(6)
N(3)–N(4)	1.373(4)	C(13)–C(15)	1.494(6)
N(4)–C(8)	1.342(5)	C(16)–C(17)	1.381(6)
N(5)–C(11)	1.347(5)	C(16)–C(19)	1.488(6)
N(5)–N(6)	1.370(4)	C(17)–C(18)	1.388(6)
N(6)–C(13)	1.339(5)	C(18)–C(20)	1.486(7)
N(1)–Pd–N(3)	89.83(12)	N(3)–Pd–N(7)	89.59(12)
N(1)–Pd–N(5)	91.03(13)	N(5)–Pd–N(7)	89.60(13)
N(1)–Pd–N(7)	178.28(12)	N(2)–Ag(1)–N(4^{I})	174.04(12)
N(3)–Pd–N(5)	178.33(13)	N(6)–Ag(2)–N(8^{I})	172.76(12)

Symmetry transformation used to generate equivalent atoms: I $-x, y, -z + \frac{1}{2}$.

bulkier Ag^+ ions leads to the formation of the $[\{PdAg_2(dmpz)_4\}_2]$ species, which crystallizes in the same $C2/c$ space group as its unsubstituted parent and possesses a dimeric molecular framework closely related to that of the hydrogen-bridged derivative. Again, the idealized molecular symmetry is 422, with the Pd and Ag atoms lying on four- and two-fold axes, respectively. Selected distances and angles are collected in Table 2, while Fig. 3 shows an ORTEP drawing of the dimer, which as for **1**, possesses crystallographic two-fold symmetry.

The steric requirements of the silver ions, *i.e.* the linear N–Ag–N co-ordination and much longer N···Ag···N distances [which lie in the range 4.152(4)–4.161(5) Å] heavily inflate the whole molecule, raising the Pd···Pd distance to 5.160(1) Å. While the local co-ordination at the Pd is only slightly deformed [Pd–N and *cis* N–Pd–N values lie in the ranges 2.008(3)–2.017(3) and 89.6(1)–91.0(1)°, respectively], several conformational parameters are changed on passing from the H^+ to the Ag^+ derivative. The most significant changes are observed in the N–Pd···Pd–N torsional angles, indicating the relative amounts of staggering of the co-ordination planes (Fig. 4) {average 68.2(1) and 84.0(1)° in $[\{Pd(dmpz)_2(Hdmpz)_2\}_2]$ **1** and $[\{PdAg_2(dmpz)_4\}_2]$ **6** respectively}; surprisingly, the dihedral angles between the dimethylpyrazolates and the PdN_4 plane [average 52.1(1) and 53.0(1)° in **1** and **6**, respectively] are only marginally changed, as if they were imposed by the steric interactions between ligands attached to the same Pd atom, rather than dictated by the nature of the dimer.

From the analysis of the aforementioned values, one can easily deduce the relatively soft motion accompanying the H/Ag substitution, as if each dimer were a molecular bellows adapting its conformation to the size of the atoms bridging the N···N vectors. Unfortunately, we could not prepare suitable crystals of the copper(I) derivative; however, as also evidenced by the isostructural relations between many simple copper(I) and silver(I) binary pyrazolates and fully organic pyrazoles,[10] it is likely that the substitution by Cu^+ yields similar dimeric molecules, probably possessing molecular features intermediate between those of **1** and **6**.

Following our previous work on binary metal pyrazolates,[15] we can now interpret the $[\{PdAg_2(dmpz)_4\}_2]$ phase as molecular crystals of a hexanuclear metal pyrazolate. Each

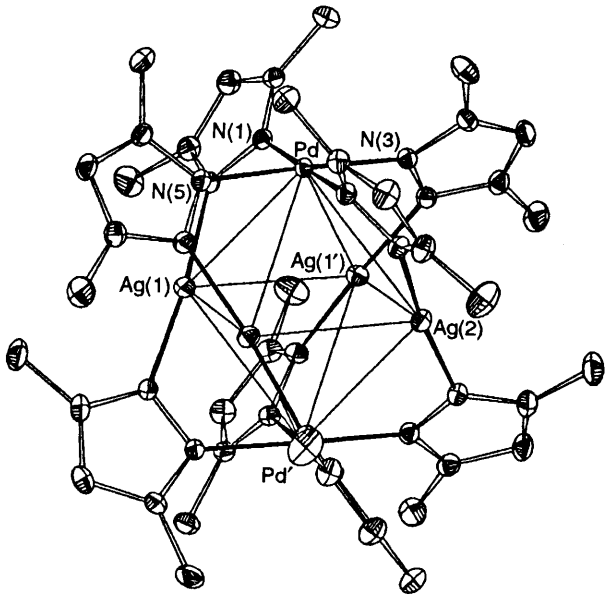

Fig. 3 An ORTEP drawing of $[\{PdAg_2(dmpz)_4\}_2]$, with the partial labelling scheme. Thermal ellipsoids are drawn at the 30% probability level

molecule, therefore, contains a metal octahedron, of *trans*-Pd_2Ag_4 formulation, bridged, on each Pd···Ag edge, by a dimethylpyrazolate ligand. Such a metal cluster, where no bonding between metal atoms occurs [Pd···Ag 3.465(1)–3.535(1), Ag···Ag 3.310(1)–3.426(1) Å], ideally contains two fused $[M(dmpz)]_4$ frameworks of idealized D_{2d} symmetry, sharing the common Pd atoms, similar to those found in the tetranuclear $[\{Cu(dppz)\}_4]$ molecule.[4] This indicates that formal substitution of linearly co-ordinated Cu, Ag and Au atoms in their tri-,[17] tetra-,[4] hexa-nuclear[17] and polymeric[15] binary pyrazolates by metals requiring a higher co-ordination number might lead to new, and unexpected, molecular arrangements, up to the formation of complex three-dimensional materials. Analogously, binary metal imidazolates containing tetra- or hexa-connected metal centres have been found to crystallize as three-dimensional solids, with complex structural features.[22]

Conclusion

The synthesis and the structural properties of a palladium(II) pyrazole/pyrazolate complex $[\{Pd(dmpz)_2(Hdmpz)_2\}_2]$ have been described. The Hdmpz ligand did not show any tendency to substitution reactions when CO or olefins were employed.[23] This inertness may be attributable to the extra stabilization of **1** because of the presence of strong intramolecular hydrogen bonds which equalize the Hdmpz and dmpz ligands. On this basis, it is unlikely that **1** will be used as a catalyst. On the contrary, complex **1** is an interesting starting material for the synthesis of heterobimetallic species, in which N–H···N groups are replaced by N–M–N groups. Studies are in progress to explore the potential of such systems, and in particular of the $[\{PdCu_2(dmpz)_4\}_2]$ species, when the interest arises because of the presence of electron-rich and electron-deficient metal centres in the same molecule.

Experimental

Pyrazole (Hpz), 3,5-dimethylpyrazole (Hdmpz), $PdCl_2$, $Na_2[PdCl_4]$, $AgNO_3$ (Aldrich Chemical Co.) and 3,5-diphenylpyrazole (Lancaster Synthesis) were used as supplied. Solvents were dried and distilled by standard methods. The complex $[PdCl_2(MeCN)_2]$ was prepared according to literature procedures.[24] Infrared spectra were recorded on a Bio-Rad-FTIR 7 instrument, NMR spectra on a Bruker WP80

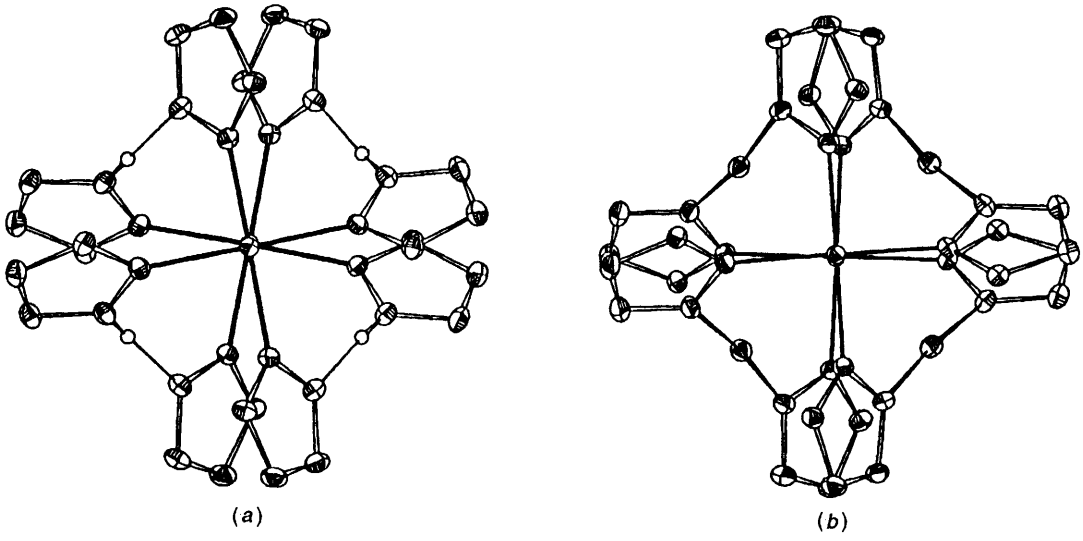

Fig. 4 Top views of $[\{Pd(dmpz)_2(Hdmpz)_2\}_2]$ (*a*) and $[\{PdAg_2(dmpz)_4\}_2]$ (*b*), showing the relative staggering of the PdN_4 co-ordination planes

spectrometer. Thermogravimetric analyses were performed on a Mettler TA4000 system. Elemental analyses were carried out at the Microanalytical Laboratory of this University.

Syntheses

$[\{Pd(dmpz)_2(Hdmpz)_2\}_2]$ 1. *Method* (*a*). To a solution of Hdmpz (0.37 g, 3.85 mmol) in methanol (8 cm^3) was added $[PdCl_2(Me_2CN)_2]$ (0.200 g, 0.77 mmol) with stirring. The pale yellow suspension was stirred for 30 min and then triethylamine (0.3 cm^3) was added. The suspension suddenly turned white. It was stirred for 4 h, and then the white solid was filtered off, washed with methanol and dried under vacuum (0.360 mg, 95%). Crystals suitable for X-ray analysis were obtained by slow evaporation of a CH_2Cl_2 solution of complex **1**.

Method (*b*). To a solution of Hdmpz (1.70 g, 17.6 mmol) in water (40 cm^3) at 60 °C was added $Na_2[PdCl_4]$ (1.00 g, 3.40 mmol) with stirring. The suspension was stirred at 60 °C for 1 h and then triethylamine (1.5 cm^3) was added. After stirring overnight at room temperature the white solid was filtered off, washed with water and methanol and dried under vacuum (1.61 g, 97%). Complex **1** was also obtained employing $PdCl_2$ in place of $Na_2[PdCl_4]$ (Found: C, 49.20; H, 6.15; N, 23.10. $C_{20}H_{30}N_8Pd$ requires C, 49.15; H, 6.15; N, 22.95%).

$[PdCl(Hdmpz)_3Cl]$ 2. To a solution of Hdmpz (0.890 g, 9.27 mmol) in diethyl ether (15 cm^3) was added $[PdCl_2(MeCN)_2]$ (0.400 mg, 1.54 mmol) with stirring. The yellow suspension slowly turned white. After 8 h the solid was filtered off, washed with diethyl ether and dried under vacuum (0.690 mg, 96%). Complexes $[Pd(Hpz)_4]Cl_2$ **4** and $[PdCl_2(Hdppz)_2]$ **5** were obtained similarly to **2**, employing Hpz or Hdppz, respectively, in place of Hdmpz. Attempts to grow crystals of **2** led invariably to the formation of $[\{PdCl_2(Hdmpz)\}_2]$ **3** (see text), even in the presence of free Hdmpz (Found: C, 38.75; H, 5.25; N, 18.10. $C_{15}H_{24}Cl_2N_6Pd$ requires C, 38.70; H, 5.20; N, 18.05%).

$[\{PdAg_2(dmpz)_4\}_2]$ 6. To a suspension of complex **1** (0.350 mg, 0.72 mequivalent) in MeCN (10 cm^3) was added $AgNO_3$ (0.370 g, 2.18 mmol) dissolved in MeCN (5 cm^3). The white suspension was left to stir for 2 h, then the solid was filtered off, washed with MeCN and dried under vacuum (0.495 g, 98%). Crystals suitable for an X-ray study were obtained by slow diffusion of pentane into a solution of **6** in CH_2Cl_2 (Found: C, 34.20; H, 3.90; N, 15.90. $C_{40}H_{56}Ag_4N_{16}Pd_2$ requires C, 34.20; H, 4.00; N, 15.95%).

$[\{PdCu_2(dmpz)_4\}_2]$ 7. To a suspension of complex **1** (0.300 g, 0.61 mequivalent) in MeCN (10 cm^3) were added, under nitrogen, $[Cu(MeCN)_4]BF_4$ (0.580 g, 1.84 mmol) and triethylamine (0.5 cm^3). The white suspension was stirred for 2 h, then the solid was filtered off under nitrogen, washed with MeCN and dried under vacuum (0.340 g, 91%) (Found: C, 38.90; H, 4.50; N, 18.05. $C_{40}H_{56}Cu_4N_{16}Pd_2$ requires C, 39.10; H, 4.55; N, 18.25%).

Reaction of complex 2 with triethylamine

To a suspension of complex **2** (0.600 g, 1.29 mmol) in methanol (10 cm^3) was added triethylamine (0.5 cm^3) with stirring. After 2 h the suspension was filtered giving 0.298 g of **1** (47% yield). Evaporation of the mother-liquors gave 0.228 g of an orange product recognized (elemental analysis and X-ray diffraction) to be *trans*-$[PdCl_2(Hdmpz)_2]$ (48% yield). When the reaction is carried out in the presence of an excess of Hdmpz, complex **1** was recovered in quantitative yield (> 95%).

Crystallography

Crystal data and experimental conditions are summarized in Table 3. Least-squares fits of the setting positions of 25 randomly oriented intense reflections with θ ranging from 10 to 12° provided the unit-cell parameters. Intensities were collected using a variable scan range with 25% extension at each end for background determination. Three standard reflections were measured at regular intervals and showed stability of the crystals over the data-collection period. All data sets were corrected for Lorentz and polarization effects. The empirical absorption correction described in ref. 25 (ψ scan; ψ = 0–360°, every 10°) was applied, using three reflections with χ near 90°.

The structures were solved by direct methods (SIR 92)[26] and Fourier-difference methods and refined by full-matrix least squares using the SHELXL 93 suite of programs,[27] locally adapted on a Silicon Graphics Indigo computer running IRIX 4.01. Scattering factors, corrected for the real and imaginary anomalous dispersion terms, were taken from the internal library of SHELXL 93. Anisotropic thermal parameters were assigned to all non-hydrogen atoms. The hydrogen-atom contribution to the scattering factors was included in the last stages of the refinement in ideal positions with a common refinable isotropic displacement parameter. In complex **1**, half-occupancy hydrogen atoms were placed on each nitrogen atom involved in hydrogen bonding. The peaks in the final Fourier-difference maps were randomly located. The final positional parameters for complexes **1** and **6** are in Tables 4 and 5, respectively.

Table 3 Summary of crystal data and structure-refinement parameters for compounds **1** and **6***

	1	**6**
Formula	$C_{40}H_{60}N_{16}Pd_2$	$C_{40}H_{56}Ag_4N_{16}Pd_2$
M	977.84	1405.29
a/Å	17.305(1)	20.843(4)
b/Å	15.737(3)	12.927(2)
c/Å	17.513(3)	19.474(3)
β/°	100.11(1)	105.22(1)
U/Å^3	4695(1)	5063(2)
F(000)	2016	2752
D_c/g cm^{-3}	1.383	1.844
μ/mm^{-1}	0.812	2.257
Crystal size/mm	0.25 × 0.10 × 0.10	0.25 × 0.22 × 0.11
Scan interval/°	0.9 + 0.35 tan θ	1.0 + 0.35 tan θ
hkl Ranges	−21 to 20, 0–19, 0–21	−24 to 23, 0–15, 0–23
Reflections collected	4602	5375
Independent reflections	4601	4434
Maximum, minimum transmission	1.00, 0.95	1.00, 0.79
Data, restraints, parameters	4597, 0, 263	4433, 0, 281
Goodness of fit on F_o^2	1.065	1.093
Final R indices [$F_o > 4\sigma(F_o)$], $R1$, $wR2$	0.0366, 0.0893	0.0258, 0.0610
(all data)	0.0492, 0.1002	0.0352, 0.0657
Maximum difference peak and hole/e Å^{-3}	0.383, −0.904	0.400, −0.535
Weighting scheme parameters a, b	0.0492, 6.1149	0.0285, 11.6364

* Details in common: monoclinic, space group $C2/c$; $Z = 4$; 293(2) K; Enraf-Nonius CAD4 diffractometer; graphite-monochromated Mo-Kα radiation (λ = 0.710 73 Å); ω scans; θ range 3–25°; 60 s (maximum) per reflection; no crystal decay; three azimuthal reflections; $w = 1/[\sigma^2(F_o^2) + (aP)^2 + bP]$, where $P = (F_o^2 + 2F_c^2)/3$; goodness of fit = $[\Sigma w(F_o^2 - F_c^2)^2/(n - p)]^{\frac{1}{2}}$ where n is the number of reflections and p the number of refined parameters; $R1 = \Sigma||F_o| - |F_c||/\Sigma|F_o|$; $wR2 = [\Sigma w(F_o^2 - F_c^2)^2/\Sigma wF_o^4]^{\frac{1}{2}}$.

Table 4 Atomic coordinates for complex **1**

Atom	x	y	z
Pd	−0.099 624(11)	0.244 186(12)	0.187 461(11)
N(1)	−0.087 17(14)	0.369 9(2)	0.169 78(14)
N(2)	−0.017 2(2)	0.403 2(2)	0.159 7(2)
N(3)	−0.153 57(14)	0.267 7(2)	0.278 33(14)
N(4)	−0.120 29(14)	0.319 8(2)	0.336 98(14)
N(5)	−0.047 44(14)	0.219 6(2)	0.095 83(13)
N(6)	0.014 11(14)	0.165 1(2)	0.101 12(14)
N(7)	−0.112 03(14)	0.118 8(2)	0.202 51(14)
N(8)	−0.083 81(14)	0.080 6(2)	0.271 61(14)
C(1)	−0.139 7(2)	0.433 8(2)	0.163 6(2)
C(2)	−0.102 3(2)	0.508 5(2)	0.148 5(2)
C(3)	−0.025 1(2)	0.487 5(2)	0.147 5(2)
C(4)	−0.224 0(2)	0.419 7(3)	0.168 1(3)
C(5)	0.042 9(3)	0.541 5(3)	0.136 1(3)
C(6)	−0.222 3(2)	0.239 0(2)	0.294 5(2)
C(7)	−0.233 2(2)	0.273 3(2)	0.364 0(2)
C(8)	−0.168 0(2)	0.323 1(2)	0.389 6(2)
C(9)	−0.275 5(2)	0.181 9(3)	0.240 7(3)
C(10)	−0.147 3(3)	0.373 9(3)	0.462 7(2)
C(11)	−0.063 1(2)	0.250 0(2)	0.023 1(2)
C(12)	−0.010 7(2)	0.213 9(2)	−0.018 7(2)
C(13)	0.037 6(2)	0.162 0(2)	0.032 0(2)
C(14)	−0.129 7(2)	0.308 7(3)	−0.003 6(2)
C(15)	0.105 3(3)	0.107 6(3)	0.019 9(3)
C(16)	−0.144 5(2)	0.058 1(2)	0.152 3(2)
C(17)	−0.137 9(2)	−0.019 1(2)	0.190 0(2)
C(18)	−0.097 8(2)	−0.003 2(2)	0.264 3(2)
C(19)	−0.182 8(2)	0.079 2(2)	0.071 0(2)
C(20)	−0.070 1(2)	−0.063 4(2)	0.329 2(2)

Table 5 Atomic coordinates for complex **6**

Atom	x	y	z
Pd	−0.117 880(13)	0.216 47(2)	0.164 609(14)
Ag(1)	−0.034 62(2)	0.085 83(3)	0.317 38(2)
Ag(2)	−0.032 66(2)	0.350 81(3)	0.318 72(2)
N(1)	−0.121 0(2)	0.061 3(2)	0.167 3(2)
N(2)	−0.093 9(2)	0.009 4(2)	0.229 3(2)
N(3)	−0.076 7(2)	0.209 1(2)	0.821(2)
N(4)	−0.019 4(2)	0.153 2(3)	0.088 4(2)
N(5)	−0.156 8(2)	0.226 2(2)	0.248 9(2)
N(6)	−0.128 5(2)	0.292 4(3)	0.303 3(2)
N(7)	−0.116 9(2)	0.372 2(2)	0.159 1(2)
N(8)	−0.060 2(2)	0.422 6(2)	0.157 1(2)
C(1)	−0.149 4(2)	−0.008 2(3)	0.117 0(2)
C(2)	−0.140 5(2)	−0.105 4(3)	0.146 5(2)
C(3)	−0.106 0(2)	−0.091 4(3)	0.217 0(2)
C(4)	−0.185 4(2)	0.023 7(4)	0.043 3(2)
C(5)	−0.084 5(3)	−0.168 5(4)	0.275 8(3)
C(6)	−0.093 8(2)	0.252 7(3)	0.017 8(2)
C(7)	−0.048 2(2)	0.224 4(4)	−0.018 7(2)
C(8)	−0.001 9(2)	0.163 5(3)	0.027 2(2)
C(9)	−0.154 6(3)	0.319 2(4)	−0.006 7(2)
C(10)	0.058 8(3)	0.110 5(5)	0.017 0(3)
C(11)	−0.212 5(2)	0.186 2(3)	0.260 8(2)
C(12)	−0.220 1(2)	0.227 3(4)	0.323 4(2)
C(13)	−0.167 3(2)	0.294 4(4)	0.348 3(2)
C(14)	−0.256 1(2)	0.112 6(4)	0.210 6(3)
C(15)	−0.149 8(3)	0.360 6(5)	0.413 4(3)
C(16)	−0.166 9(2)	0.441 2(3)	0.149 7(2)
C(17)	−0.141 8(2)	0.537 8(3)	0.141 4(3)
C(18)	−0.074 6(2)	0.523 7(3)	0.146 6(3)
C(19)	−0.236 0(2)	0.410 9(4)	0.148 9(3)
C(20)	−0.022 7(3)	0.598 6(4)	0.139 5(4)

Complete atomic coordinates, thermal parameters and bond lengths and angles have been deposited at the Cambridge Crystallographic Data Centre. See Instructions for Authors, *J. Chem. Soc., Dalton Trans.*, 1996, Issue 1.

Acknowledgements

This work was supported by the Italian Consiglio Nazionale delle Ricerche (CNR, Progetto Finalizzato Chimica Fine II) and by the Ministero dell'Università e della Ricerca Scientifica e Tecnologica (MURST). G. A. A. and G. L. M. thank the Istituto di Scienze Matematiche, Fisiche e Chimiche, Como, for leave. The technical support of Mr. G. Mezza is also acknowledged.

References

1 S. Trofimenko, *Prog. Inorg. Chem.*, 1986, **34**, 115.
2 See, for example, D. Röttger, G. Erker, M. Grehl and H. Fröhlich, *Organometallics*, 1994, **13**, 3897; C. W. Eigenbrot, jun., and K. N. Raymond, *Inorg. Chem.*, 1982, **21**, 2653; A. Podder, J. K. Dattagupta and N. Saha, *Acta Crystallogr., Sect. A*, 1984, **40**, C301; G. B. Deacon, B. M. Gatehouse, S. Nickel and S. N. Platts, *Aust.*

J. Chem., 1991, **44**, 613; H. Schumann, P. R. Lee and J. Loebel, *Angew. Chem., Int. Ed. Engl.*, 1989, **26**, 1033; J. E. Cosgriff, G. B. Deacon, B. M. Gatehouse, H. Hemling and H. Schumann, *Angew. Chem., Int. Ed. Engl.*, 1993, **32**, 874; J. E. Cosgriff, G. B. Deacon and B. M. Gatehouse, *Aust. J. Chem.*, 1993, **46**, 1881.
3 G. A. Ardizzoia, M. Angaroni, G. La Monica, N. Masciocchi and M. Moret, *J. Chem. Soc., Dalton Trans.*, 1990, 2277; N. Masciocchi, M. Moret, G. A. Ardizzoia and G. La Monica, in *The Chemistry of Copper and Zinc Triads*, eds. A. J. Welch and S. K. Chapman, Royal Society of Chemistry, Cambridge, 1993, p. 129; G. A. Ardizzoia and G. La Monica, *Inorg. Synth.*, in the press.
4 G. A. Ardizzoia, M. Angaroni, G. La Monica, F. Cariati, S. Cenini, M. Moret and N. Masciocchi, *Inorg. Chem.*, 1991, **30**, 4347; G. A. Ardizzoia, S. Cenini, G. La Monica, N. Masciocchi and M. Moret, *Inorg. Chem.*, 1994, **33**, 1458.
5 W. Burger and J. Z. Strähle, *Z. Anorg. Allg. Chem.*, 1986, **539**, 27.
6 D. Carmona, L. A. Oro, M. P. Lamala, J. Elguero, M. C. Apreda, C. Foces-Foces and F. H. Cano, *Angew. Chem., Int. Ed. Engl.*, 1986, **25**, 1114.
7 M. K. Ehlert, S. J. Rettig, A. Storr, R. C. Thompson and J. Trotter, *Can. J. Chem.*, 1990, **68**, 1494.
8 M. K. Ehlert, S. J. Rettig, A. Storr, R. C. Thompson and J. Trotter, *Can. J. Chem.*, 1993, **71**, 1425.
9 J. Roziere and J. Potier, *J. Inorg. Nucl. Chem.*, 1973, **35**, 1179.
10 J. Berthou, J. Elguero and C. Rerat, *Acta Crystallogr., Sect. B*, 1970, **26**, 1880; F. Krebs Larsen, M. S. Lehmann, I. Sotofte and S. E. Rasmussen, *Acta Chem. Scand.*, 1970, **24**, 3248; A. Baldy, J. Elguero, R. Faure, M. Pierrot and E. J. Vincent, *J. Am. Chem. Soc.*, 1985, **107**, 5290; J. A. S. Smith, D. Wehrle, F. Aguilar-Parrilla, H. H. Limbach, M. Foces-Foces, F. H. Cano, J. Elguero, A. Baldy, M. Pierrot, M. M. T. Khursid and J. B. Larcombe-McDouall, *J. Am. Chem. Soc.*, 1989, **111**, 7304; E. N. Maslen, J. R. Cannon, A. H. White and A. C. Willis, *J. Chem. Soc., Perkin Trans.*, 1974, 1298; F. H. Moore, A. H. White and A. C. Willis, *J. Chem. Soc., Perkin Trans.*, 1975, 1068; F. Aguilar-Parrilla, G. Scherer, H. H. Limbach, M. Foces-Foces, F. H. Cano, J. A. S. Smith, C. Toiron and J. Elguero, *J. Am. Chem. Soc.*, 1992, **114**, 9657; F. Aguilar-Parrilla, C. Cativiela, M. D. Diaz de Villegas, J. Elguero, C. Foces-Foces, J. I. Garcia Laureiro, F. H. Cano, H. H. Limbach, J. A. S. Smith and C. Toiron, *J. Chem. Soc., Perkin Trans.*, 1992, 1737; C. Foces-Foces, F. H. Cano and J. Elguero, *Gazz. Chim. Ital.*, 1993, **123**, 477; A. L. Llamas-Saiz, C. Foces-Foces, I. Sobrados, J. Elguero and W. Meutermans, *Acta Crystallogr., Sect. C*, 1993, **49**, 724; R. G. Raptis, R. J. Staples, C. King and J. P. Fackler, jun., *Acta Crystallogr., Sect. C*, 1993, **49**, 1716.
11 F. H. Moore, K. A. White and A. C. Willis, *J. Chem. Soc., Perkin Trans. 2*, 1975, 1068.
12 C. K. Johnson, ORTEP II, Report ORNL-3794 (revised), Oak Ridge National Laboratory, Oak Ridge, TN, 1971.
13 C. H. Cheng, J. S. Lain, Y. J. Wu and S. L. Wang, *Acta Crystallogr., Sect. C*, 1990, **46**, 208.
14 G. Minghetti, G. Banditelli and F. Bonati, *Can. J. Chem.*, 1979, **57**, 1851.
15 N. Masciocchi, M. Moret, P. Cairati, A. Sironi, G. A. Ardizzoia and G. La Monica, *J. Am. Chem. Soc.*, 1994, **116**, 7668.
16 M. K. Ehlert, S. J. Rettig, R. C. Thompson and J. Trotter, *Can. J. Chem.*, 1989, **67**, 1970; 1991, **69**, 432.
17 M. K. Ehlert, S. J. Rettig, A. Storr, R. C. Thompson and J. Trotter, *Can. J. Chem.*, 1990, **68**, 1444; R. G. Raptis and J. P. Fackler, jun., *Inorg. Chem.*, 1988, **27**, 4179; R. G. Raptis, H. H. Murray and J. P. Fackler, jun., *Inorg. Chem.*, 1988, **27**, 26; *J. Chem. Soc., Chem. Commun.*, 1987, 737; B. Bovio, F. Bonati and G. Banditelli, *Inorg. Chim. Acta*, 1984, **87**, 25.
18 A. C. Skapski and M. L. Smart, *Chem. Commun.*, 1970, 658.
19 W. Burger and J. Strähle, *Z. Anorg. Allg. Chem.*, 1985, **529**, 111.
20 S. Trofimenko, *Chem. Rev.*, 1972, **72**, 497.
21 F. D. Rochon and R. Melanson, *Acta Crystallogr., Sect. B*, 1981, **37**, 690.
22 J. A. J. Jarvis and A. F. Wells, *Acta Crystallogr.*, 1960, **13**, 1027; M. Sturm, F. Brandl, D. Engel and W. Hoppe, *Acta Crystallogr., Sect. B*, 1975, **31**, 2369; R. Lehnert and F. Seel, *Z. Anorg. Allg. Chem.*, 1980, **464**, 187; A. L. Spek, J. M. Duisenberg and M. C. Feiters, *Acta Crystallogr., Sect. C*, 1983, **39**, 1212.
23 G. A. Ardizzoia, G. La Monica, S. Cenini, N. Masciocchi and M. Moret, unpublished work.
24 J. R. Doyle, P. E. Slade and H. B. Jonassen, *Inorg. Synth.*, 1969, **6**, 216.
25 A. C. T. North, D. C. Phillips and F. S. Mathews, *Acta Crystallogr., Sect. A*, 1968, **24**, 351.
26 A. Altomare, G. Cascarano, C. Giacovazzo, A. Guagliardi, M. C. Burla, G. Polidori and M. Camalli, *J. Appl. Crystallogr.*, 1994, **27**, 435.
27 G. M. Sheldrick, SHELXL 93, Program for the Refinement of Crystal Structures, University of Göttingen, 1993.

Received 31*st August* 1995; *Paper* 5/05748E